Pionic transparency in semi-exclusive electroproduction off nuclei

Murat M. Kaskulov,* Kai Gallmeister, and Ulrich Mosel
Institut für Theoretische Physik, Universität Giessen, Germany
(Dated: January 24, 2021)

We investigate the early onset of pionic color transparency (πCT) observed at Jefferson Laboratory (JLAB) in semi–exclusive pion electroproduction reaction $A(e,e'\pi^+)$ off nuclei. In the present description the primary $\gamma^* p \to \pi^+ n$ interaction is described very well both for the longitudinal and the transverse polarizations. For the final state interactions a coupled–channel treatment of the interactions of transmitted hadrons allows to go beyond the Glauber approximation. We show that a proper distinction between the soft hadronic and hard partonic components of the electroproduction amplitude is essential for a quantitative description of the measured nuclear transparency. The data are well reproduced if one assumes that point–like configurations are produced in the regime of hard deep–inelastic scattering (DIS) off partons and dominate the transverse channel.

PACS numbers: 25.20.Lj, 13.75.Gx, 12.39.Fe, 11.80.La, 13.40.Gp

The interactions of high–energy virtual photons with nuclei provide an important tool to study the early stage of hadronization and (pre)hadronic final–state–interactions (FSI) at small distances $d \sim 1/\sqrt{Q^2}$. A further advantage of lepton–induced reactions is that one may vary the energy ν and virtuality Q^2 of the incident photon independently of each other. This allows to study the phenomenon of Color Transparency (CT) [1, 2], i.e. the reduced interaction cross section of a small sized color singlet object produced in processes at high momentum transfer. Furthermore, in the kinematic regime where one is less sensitive to the resolved hadronic interactions of photons – coherence length effect – the photonuclear reactions are not contaminated by initial–state–interactions (ISI). This is an advantage compared to the use of hadronic projectiles, which are strongly shadowed on their way to the reaction point inside the nucleus.

In the presence of the CT effect the intranuclear attenuation of hadrons propagating through the nuclear medium should decrease as a function of photon virtuality Q^2. In this case the nucleus becomes more transparent for the outgoing particles as compared to the case where the attenuation is driven by ordinary absorption mechanisms. One may use a transparency ratio[1] as a tool to search for deviations from predictions of models based on conventional nuclear many–body mechanisms.

During the last decade, a number of experiments have been performed to measure the nuclear transparencies in search of CT. These include the measurements of transparencies in reactions $A(p,2p)$ [3, 4, 5, 6], $A(e,e'p)$ [7, 8, 9, 10, 11, 12], ρ–meson electroproduction off nuclei [13, 14], π–photoproduction [15], coherent diffractive dissociation of pions into di–jets [16]. We refer to Ref. [17], where a summary of the possible signatures of CT in these reactions can be found.

It is expected that CT should be more pronounced in reactions involving mesons instead of baryons. Indeed, it might appear more probable to produce a two–quark system with a small transverse size and, as a consequence, reduced FSI. This idea had been followed by the HERMES experiment on ρ–meson production on nuclei [14] which seemed to indicate CT effects. Subsequent theoretical analyses of this experiment did show, however, that the effects of CT could not be clearly distinguished from those of shadowing in the entrance channel [18, 19]. The latter calculation [19] showed that it is essential in any analysis of the CT effect to properly account for FSI and experimental acceptance limitations. The coherence length has been kept approximately constant in an experiment at JLAB [20] where the nuclear transparency in semi–exclusive π^+ electroproduction reaction $A(e,e'\pi^+)$ has been measured as a function of Q^2 and the atomic mass number A, a rise of pionic transparency has been observed for values of Q^2 between 1 and 5 GeV^2. Since the π–nucleon cross section is nearly constant for energies covered by the experiment, transparencies calculated in the standard Glauber model are independent of Q^2. The observed Q^2 dependence of the π^+ transparency deviates from the calculations without CT of Refs. [21, 22], and is in fair agreement with the calculations of the same groups when including CT. In Ref. [21] a semiclassical model for FSI has been used, while in Ref. [22] a relativistic version of the Glauber model has been developed. Both groups incorporate CT using the quantum diffusion picture [23].

In this work we study the onset of CT at JLAB using a factorization of the whole reaction into an initial, primary interaction of the incoming virtual photon with the nucleon and the FSI. The cross section for the former is reproduced both in its longitudinal and its transverse contribution while the FSI is treated within transport approach. The main advantage of the present approach to FSI is its universality and a use of input parameters already tested in many different kinds of nuclear reactions, for example, for photo– and electropro-

*Electronic address: kaskulov@theo.physik.uni-giessen.de

[1] The nuclear transparency for a certain reaction process is usually defined as the ratio of the nuclear cross section per target nucleon to the one for a free nucleon, i.e. $T_A = \sigma_A/A\sigma_N$.

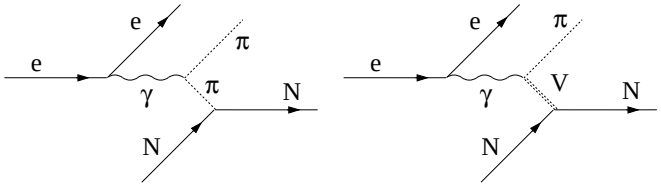

FIG. 1: The diagrams describing the hadron–exchange part of the π^+– electroproduction amplitude. See text for the details.

duction reactions [24]. For the present investigation the studies of pion–processes in nuclei are particularly relevant [25, 26]. Because our calculations represent a complete event simulation it is possible to take experimental acceptance effects into account. In the following we carry out the transport MC simulation using the actual acceptance conditions of the πCT experiment at JLAB [20, 27]. As a central result we will show that a quantitative understanding of the observed nuclear transparency requires a detailed understanding of the primary, elementary (γ^*, π^+) reaction on the proton. In spite of the fact that the results of Refs. [21, 22] do provide a rather strong support for the CT we further show that because of large uncertainties in the formation time concepts the longitudinal–transverse (L–T) separated nuclear cross sections are needed for a quantitative understanding and proof of the CT effect.

The calculations of Refs. [21, 22] mainly deal with effects of FSI and do not account for many features of the (γ^*, π^+) reaction amplitude. Our interpretation of the πCT data is closely tied to a microscopic model for the primary reaction $p(e, e'\pi^+)n$. At first we briefly describe the model for the exclusive process

$$\gamma^*(q) + N(p) \to \pi(k') + N'(p'). \qquad (1)$$

Following Ref. [28] we distinguish two classes of primary collisions: a soft hadronic and a hard partonic (DIS) production of π^+. The soft hadron–exchange part of the $\gamma^* p \to n\pi^+$ amplitude is described by the exchange of Regge trajectories [29]. The Feynman diagrams are shown in Figure 1. The left diagram in Figure 1 corresponds to the exchange of the π–Regge trajectory and

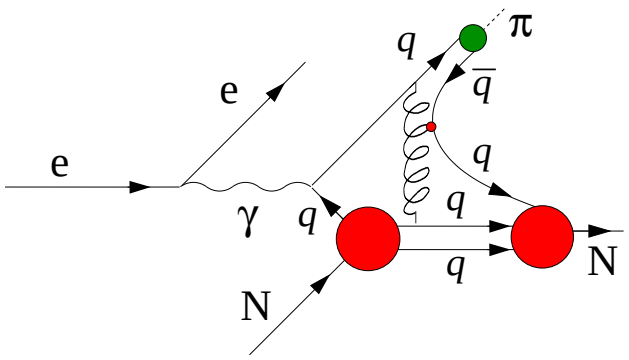

FIG. 2: A schematic representation of the partonic DIS part of the π^+– electroproduction mechanism. The wavy line represents a color string. See text for the details.

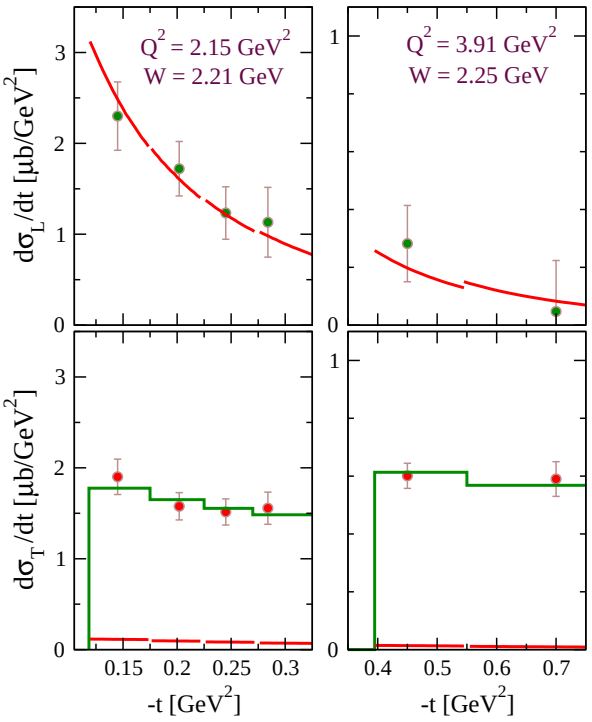

FIG. 3: The longitudinal $d\sigma_L/dt$ (top panels) and transverse $d\sigma_T/dt$ (bottom panels) differential cross sections of the reaction $p(e, e'\pi^+)n$ at average values of $Q^2 = 2.15$ GeV^2 and $Q^2 = 3.91$ GeV^2. The solid curves are the contribution of the hadron–exchange model and the histograms are the contribution of the DIS pions. The πCT data are from Ref. [36]. The discontinuities in the curves result from the different values of Q^2 and W for the various $-t$ bins.

is referred as the π^+ quasi–elastic knockout mechanism. The latter also contains the electric part of the s–channel nucleon Born term to conserve the charge of the system. The right diagram in Figure 1 describes the exchange of the ρ–meson Regge trajectory and gives only a marginal contribution to the cross section. The corresponding gauge invariant hadronic currents and parameters of the Regge trajectories are given in Ref. [28].

At the invariant masses reached in the πCT experiment ($W \approx 2.2$ GeV) nucleon resonances can contribute to the 1π channel. As in Ref. [28] this is modeled by the hard interaction of virtual photons with partons (DIS) since DIS involves all possible transitions of the nucleon from its ground state to any excited state [30]. For the proper description of the reaction $p(e, e'\pi^+)n$ in DIS a model for the hadronization process is needed. In the present description of the hadronization in DIS we rely on the Lund fragmentation model [31] as depicted in Figure 2 where the leading order $\gamma^* q \to q$ DIS process followed by the fragmentation of an excited string into two particles (πN) is shown. As a realization of the Lund model we use the JETSET implementation [32]. We note that this description resolves the longstanding puzzle of a large theoretical underestimate of the observed transverse strength in the model of [29].

In the calculation presented in Ref. [28] the transverse part is solely generated by the DIS process. However, contrary to the situation at higher values of Q^2 considered in Ref. [28] where the hadronic part gives only a marginal contribution to $\sigma_{\rm T}$, at low Q^2 the problem of double counting arises when using both the DIS and the Regge contributions to the transverse cross section. Following Ref. [33] this could be solved by turning off the leading order DIS contribution, as required by gauge invariance for $\gamma^* q \to q$, when approaching the photon point where the Regge description alone gives a good description of data [29]. Therefore, an additional empirical factor [33]

$$Q^4/(Q^2+\Lambda^2)^2 \qquad (2)$$

is introduced into the DIS cross section with the cut–off Λ as a fit parameter. This factor is $\simeq 1$ at high values of Q^2 and tends to zero at small values of Q^2. The combined description of data from the JLAB $F\pi$–1 experiment [34] at low values of Q^2 and $F\pi$–2 experiment [35] at high Q^2 results in $\Lambda \simeq 400$ MeV. In the Q^2 range considered in Ref. [28] Eq. (2) is close to unity and is largely ineffective for the results presented there.

In Figure 3 the results for the $p(\gamma^*,\pi^+)n$ differential cross sections $d\sigma_{\rm L}/dt$ (top panels) and $d\sigma_{\rm T}/dt$ (bottom panels) are compared with the πCT data of Ref. [36]. The longitudinal cross section $d\sigma_{\rm L}/dt$ is very well described by the hadron–exchange model (solid curves). The discontinuities in the curves result from the different values of Q^2 and W for the various $-t$ bins. The steep fall of $d\sigma_{\rm L}/dt$ away from forward angles comes entirely from the rapidly decreasing π–pole amplitude. The lower part of Figure 3 shows that the transverse cross section can be readily explained [28] by a contribution from DIS pions (solid histograms). In the present paper the model of Ref. [28] provides an accurate representation of the elementary (γ^*,π^+) cross section.

In Figure 4 (left panel) we show the integrated (γ^*,π^+) cross sections. At given $W = 2.2$ GeV the hard partonic part of the cross section (dash-dotted curve) dominates the π^+ production mechanism. However, what matters in the πCT experiment is the forward production, since the experiment has been done at parallel kinematics with $\vec{q} \parallel \vec{k}'$. In this kinematical regime the situation is opposite and the soft π^+ quasi–elastic knockout mechanism (dashed and solid curves correspond to the longitudinal and transverse components, respectively) dominates up to $Q^2 \approx 3$ GeV^2, as shown in the right panel of Figure 4. As we shall see, this complex interplay between soft hadronic and hard partonic components of the (γ^*,π^+) reaction is crucial for the interpretation of πCT data.

Concerning the overall reaction mechanisms on *nuclei* we rely on a separation of different processes. At first (in the impulse approximation) the e–beam interacts with a nucleon inside the nucleus. It is supposed that the elementary interaction with nucleon is the same as that with a free nucleon. All the standard nuclear effects like

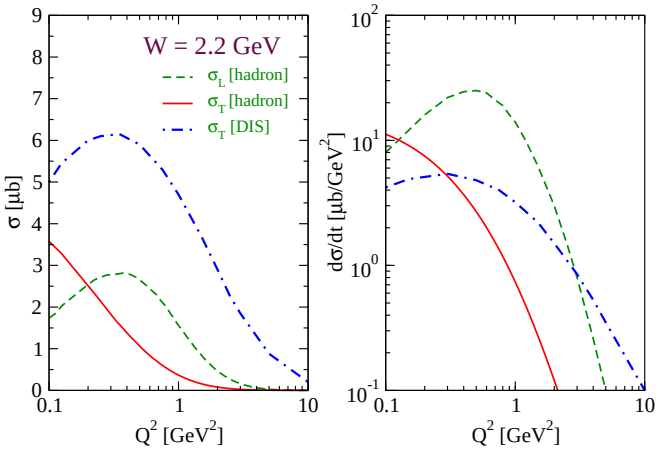

FIG. 4: Left panel: Decomposition of the the integrated virtual photon–nucleon cross sections of the exclusive reaction $p(e,e'\pi^+)n$ as a function of the photon virtuality Q^2 at $W = 2.2$ GeV. The contribution of the hadron–exchange model to the transverse $\sigma_{\rm T}$ and longitudinal $\sigma_{\rm L}$ cross sections are shown by solid and dashed curves, respectively. The contribution of DIS pions to $\sigma_{\rm T}$ is shown by the dash–dotted curve. Right panel: The forward π^+ differential cross sections as a function of Q^2.

Fermi motion, Pauli blocking and nuclear shadowing are properly taken into account. In a second step, all produced (pre)hadrons are propagated through the nuclear medium according to the transport equation.

A necessary condition for the CT effect is the propagation of a quark–gluon system, originating in the hard partonic interaction, through the nuclear medium and its subsequent interactions with surrounding nucleons. In the present model the hard DIS part of the primary high energy electromagnetic interaction is determined by the Lund model which means that the final state consists of an excited string (see Figure 2). This string then fragments into hadrons. Following Ref. [37] we extract *production* and *formation* times t_P and t_F of hadrons in the target rest frame from the MC calculation. We note however, that in the fragmentation of a string into two particles all parameters are fixed and the times may be extracted analytically. In the exclusive reaction $(e,e'\pi^+)$ considered here all pions are – because of their high energy $z \approx 1$ – directly connected to the hard interaction point and thus have production time $t_P = 0$. The Lund model formation times of exclusive (pre)pions in the forward kinematics of the πCT experiment are shown in Figure 5 (solid curve) and include the dilatation effect in the target rest frame; they are close to zero in the hadron's rest frame. At the highest Q^2 the corresponding formation lengths in the laboratory (the rest frame of the target nucleus) exceed the nuclear radius so that this effect alone already leads to an increase of transparency with Q^2.

As a second possible scenario we compare the Lund model *formation* time t_F in the laboratory with the estimate used in Ref. [21]. In this work the characteristic time t_F needed to evolve the (pre)pion to its physical

state is given by [23]

$$t_F \simeq \frac{1}{\sqrt{m_\pi^{*2}+(\vec{k}')^2}-\sqrt{m_\pi^2+(\vec{k}')^2}} \approx \frac{2|\vec{k}'|}{m_\pi^{*2}-m_\pi^2}. \quad (3)$$

where $\vec{k}'$ is the three momentum of the outgoing pion and the last approximation is valid only for the ultra-relativistic hadrons. In the rest frame of the (pre)hadron, *i.e.* $\vec{k}' = 0$ one gets a well known result $\tau_F = 1/\Delta M$ where $\Delta M = m_\pi^* - m_\pi$ is given by the lowest lying Regge partner of mass m_π^*. Although, in the original work [23] a rather small value of $\Delta M^2 \simeq 0.25$ GeV^2 has been suggested, in Ref. [21] two values were considered $\Delta M^2 = 1.4$ GeV^2 and $\Delta M^2 = 0.7$ GeV^2. Clearly, as pointed out in [23] all the above estimates can be considered as educated guesses at best. For instance, the value of $\Delta M^2 = 1.4$ GeV^2 corresponds to the expansion time in the rest frame $\tau_F = 0.16$ fm. This has to be compared with the Lund model which gives the following estimate for the *formation* time τ_F in the rest frame of the (pre)pion

$$\tau_F \simeq \frac{m_\pi}{\kappa}\frac{1}{z} \approx 0.14 \text{ fm}, \quad (4)$$

where $z \approx 1$ and a string tension $\kappa = 1$ GeV/fm. A direct extraction of τ_F from MC [37] gives $\tau_F = 0.17$ fm. However, the corresponding times in the laboratory t_F are very different. As one can see in Figure 5 in the Lund model the *formation* time t_F (solid curve) is by about factor of 3 bigger than t_F obtained when using Eq. (3) (dashed curve). The reason for such differences is related to the fact that in the Lund model the decay products of the excited strings are projected onto the states with physical masses and a notion of excited (pre)hadrons with large masses which then turn in time into the physical ones is not realized in this scheme. In particular, what is essentially time dilated in the Lund scheme is the (pre)hadron with the physical mass of the hadron.

We further use the quantum diffusion model of Ref. [23] to describe the time–development of the interactions of a point–like configuration produced in a hard initial reaction. This approach combines a linear increase of the

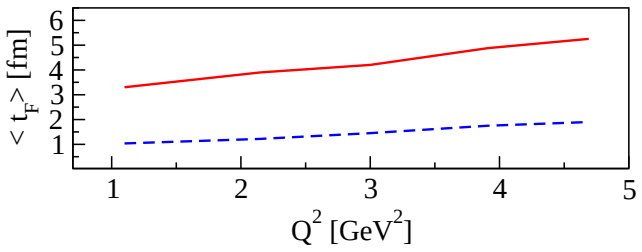

FIG. 5: The Lund model average formation time of (pre)pions (solid curve) in the target rest frame as a function of Q^2 in the forward kinematics of the πCT experiment. The dashed curve is an estimate based on Eq. (3) with $\Delta M^2 = 1$ GeV^2.

Q^2 GeV^2	ν GeV	W GeV	$-t$ GeV^2	θ_γ deg	$\lvert\vec{k}'\rvert$ GeV	$\lvert\vec{k}\rvert$ GeV	ε	x_B	l_h fm
1.10	2.831	2.26	0.050	10.58	2.793	0.23	0.50	0.21	0.67
2.15	3.282	2.21	0.158	13.44	3.187	0.41	0.56	0.35	0.49
3.00	3.582	2.14	0.289	12.74	3.418	0.56	0.45	0.45	0.41
3.91	4.344	2.26	0.413	11.53	4.077	0.70	0.39	0.50	0.39
4.69	4.733	2.25	0.527	9.09	4.412	0.79	0.26	0.54	0.36

TABLE I: The central kinematics of the πCT experiment in the laboratory [27]. Here t and $|\vec{k}|$ stand for the four and three momentum transfer to the target, respectively, θ_γ is the angle between the three momentum of the virtual photon and the electron beam direction in the laboratory, ε is the virtual photon polarization, the Bjorken variable $x_B = Q^2/2M_N\nu$ and l_h denotes the coherence length for each kinematics settings. For the parallel kinematics $\theta_\gamma = \theta_\pi$ where θ_π is the angle of the emitted pion with three momentum $|\vec{k}'|$.

hadron–nucleon cross section with the assumption that the cross section for the leading particles does not start at zero, but at a finite pedestal value connected with Q^2 of the initial interaction, *i.e.*

$$\sigma^*(t)/\sigma = X_0 + (1-X_0)\left((t-t_P)/(t_F-t_P)\right), \quad (5)$$

where $X_0 = r_{\rm lead}\frac{const}{Q^2}$ with $r_{\rm lead}$ standing for the ratios of leading partons over the total number of partons (2 for mesons, 3 for baryons). The baseline value X_0 is inspired by the coefficient $n^2\langle k_t^2\rangle/Q^2$ in [23], where $n = 2$ for mesons and $\langle k_t^2\rangle$ denotes the average transverse momentum of partons. The scaling with $r_{\rm lead}$ guarantees that summing over all particles in an event, on average the prefactor becomes unity. The size of the pion enters through the (pre)hadronic cross sections with the pedestal $1/Q^2$ behavior and also through the linear rise of the (pre)hadronic interaction cross section. Using Eq. (5) the (pre)hadronic cross section is zero before the *production* time t_P and equals the full hadronic cross section after the *formation* time t_F. We note that, following the Lund model hadronization pattern this (pre)hadronic interaction is effective only for the DIS events; the longitudinal cross section is not affected by this (pre)hadronic interaction. Thus, in the model of Ref. [28] only the DIS (transverse) part of the cross section is responsible for the observed effect since this part is connected with the 4D pattern of the string breaking dynamics which makes the formation time of (pre)hadrons finite.

The propagation of the produced (pre)hadron through the nuclear medium is described by the Boltzmann–Uehling–Uhlenbeck (BUU) equation which describes the time evolution of the phase space density $f_i(\vec{r},\vec{p},t)$ of particles of type i that can interact via binary reactions. Besides the produced hadron and the nucleons these particles involve the baryonic resonances and mesons that can be produced in FSI. For the baryons the equation contains a mean field potential which depends on the particle position and momentum. The BUU equations of each particle species i are coupled via the mean field and the collision integral. The latter allows for elastic and

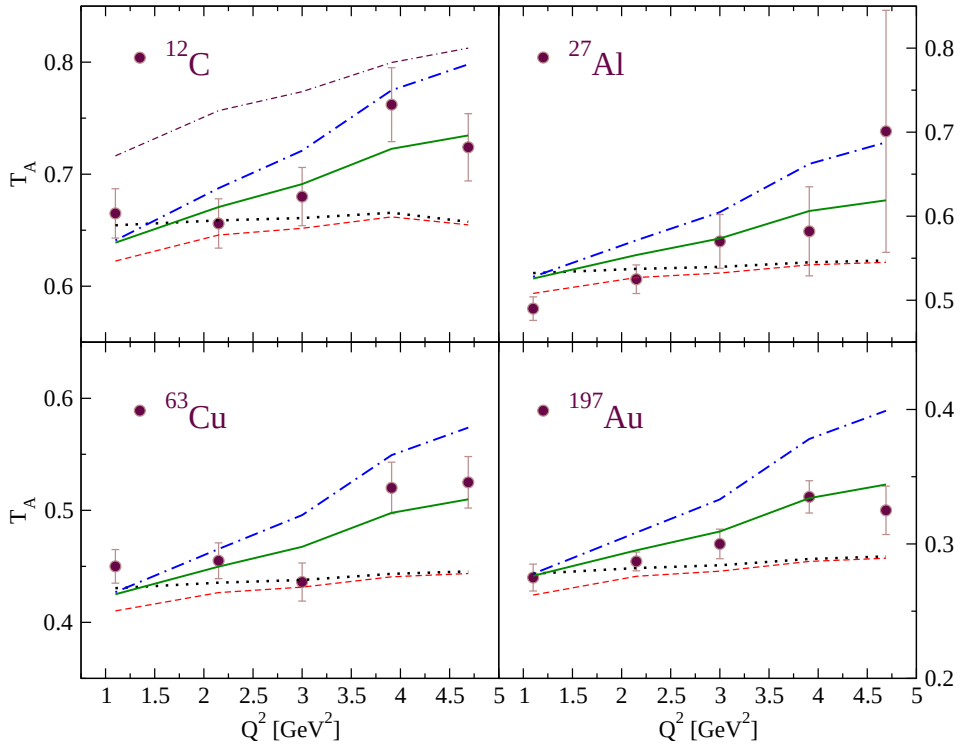

FIG. 6: Transparency, T_A, vs. Q^2 for ^{12}C (left, top panel), ^{27}Al (right, top), ^{63}Cu (left, bottom) and ^{197}Au (right, bottom). The dotted curves correspond to FSI with the full hadronic cross section and the dashed curves include the shadowing corrections. The dash–dotted curves correspond to the in–medium cross sections defined according to the Lund model formation time concept which includes the Q^2–dependent (pre)hadronic interactions, Eq. (5), for the transverse contribution. The solid curves describe the effect of time dilatation alone with the pedestal value in the effective cross section independent of Q^2. The dash–dash–dotted curve in the top left panel realises the CT effect both in the longitudinal and transverse channels. The experimental data are from Ref. [20].

inelastic rescattering and side–feeding through coupled–channel effects; it accounts for the creation and annihilation of particles of type i in a secondary collisions as well as elastic scattering from one position in phase space into another. The resulting system of coupled differential–integral equations is solved via a test particle ansatz for the phase space density. For fermions Pauli blocking is taken into account via blocking factors in the collision term [38]. We note that exactly this method leads to a good simultaneous description of hadronic attenuation in nuclei observed both by the EMC (200 GeV) and the HERMES (27 GeV) experiments [39]. The model also works very well for semi–exclusive reactions as has been shown, for example, in analysis of the photoproduction of mesons on nuclei [26, 40]. In [26] it has been shown, that for pions coherent production, which is outside the applicability of semiclassical transport, does not play a role above the $\Delta(1232)$–resonance.

Following Ref. [20] the nuclear transparency ratio in the reaction $A(e,e'\pi^+)$ is defined as

$$T_A = \sigma_A^{\rm FSI}/\sigma_A, \tag{6}$$

where the cross sections σ_A (in the laboratory) read

$$\sigma_A = \int_{\Delta M_X} dM_X \frac{d\sigma_A}{dQ^2 d\nu d\Omega_\pi dM_X}. \tag{7}$$

In Eq. (6) $\sigma_A^{\rm FSI}$ and σ_A are the results of the model calculations with and without FSI of hadrons in their way out of the nucleus, respectively. In Eq. (7) M_X stands for the missing mass of the recoiling nuclear system. It can be calculated using the four momenta of the virtual photon q and the four momentum of the detected pion k': $M_X^2 = (q + P_A - k')^2$, where $P_A = (M_A, \vec{0})$ denotes the four momentum of the nuclear target in the laboratory. In Eq. (7) ΔM_X denotes the region of the missing mass M_X within the experimental acceptance. In the case of the free proton target, the missing mass is a δ–function at the neutron mass. For nuclei, the Fermi motion of the bound nucleons broadens the distributions, and the missing mass is limited by the acceptance conditions. The lower limit of M_X is fixed by the 1π production threshold and the upper limit of M_X in the integration is determined by the values imposed in the actual experiment. The latter is done to reduce the contamination from multi–pion events in the final yield. This guarantees that in the simulation procedure, like in the actual experiment, one selects events containing only single π^+ and the residual excited nucleus. The positions of the above–threshold nuclear missing mass cuts for all the kinematic settings (see Table I) and targets are taken from Ref. [27] and used in the calculations.

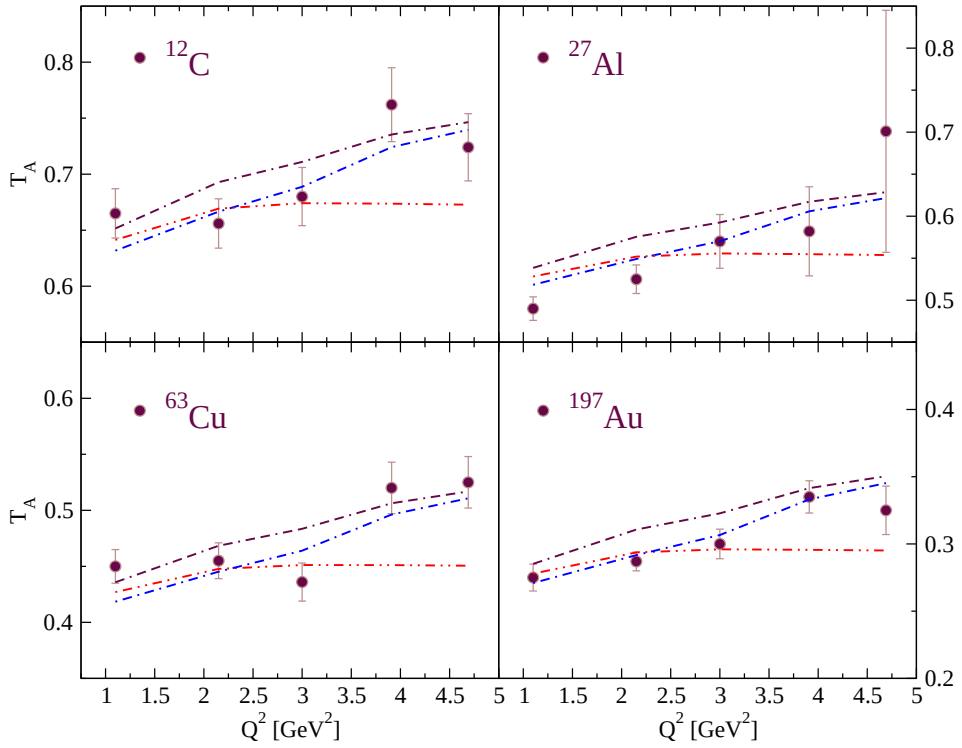

FIG. 7: Transparency, T_A, vs. Q^2 for ^{12}C (left, top panel), ^{27}Al (right, top), ^{63}Cu (left, bottom) and ^{197}Au (right, bottom). The formation time of (pre)pions in the laboratory is calculated using Eq. (3). The dash–dash–dotted curves realize the CT effect in both the longitudinal and transverse channels and dash–dotted curves in the transverse channel only. The dot–dot–dashed curves describe the CT effect in the longitudinal channel only. The experimental data are from Ref. [20].

Note that the shadowing (ISI) of the virtual photon is rather small for the kinematic conditions of the πCT experiment and varies weakly with Q^2. The coherence length $l_h \simeq 2\nu/Q^2 + m_h$, where m_h stands for the mass of the ρ–meson, varies (see Table I) from $\simeq 0.67$ fm at $Q^2 = 1.1$ GeV^2 down to 0.36 fm, *i.e.* less than one nucleon's radius, at $Q^2 = 4.69$ GeV^2, only. The ISI effect for the VMD like π^+ quasi–elastic knockout part is included in the numerator of Eq. (6) using the method of Ref. [19].

We have performed the calculations for the nuclei ^{12}C, ^{27}Al, ^{64}Cu and ^{197}Au at identical kinematics shown in Table I. Here the central values correspond to the parallel kinematics ($\theta_\gamma = \theta_\pi$) where the magnitude of the outgoing pion three momentum $|\vec{k}'|$ is given by

$$|\vec{k}'| = \sqrt{Q^2 + \nu^2} - |\vec{k}|, \qquad (8)$$

where $|\vec{k}|$ is the three momentum transfer to the nucleus. The parallel kinematics $\vec{q} \parallel \vec{k}'$ is supposed to minimize the contribution of the elastic rescattering [17].

In Figure 6 we show our results with different scenarios for the hadronic FSI. At first, we consider a case where all the produced hadrons interact from their production on with the full hadronic cross sections. The result of this calculation is shown by the dotted curves. These curves are nearly flat and thus do not exhibit the observed rise with Q^2. The same is true for the short–dashed curves which include in addition the ISI shadowing; the influence of the latter is very small due to the very small coherence lengths as discussed above.

The dash–dotted curves in Figure 6 correspond to the in–medium cross sections defined according to the Lund model formation time concept which includes the Q^2–dependent (pre)hadronic interactions, Eq. (5), for the transverse contribution. Here the pedestal value X_0 has been fixed by assuming $\sqrt{\langle k_t^2 \rangle} = 350$ MeV, i.e. the value used in the studies of [21, 22]. This model reproduces the trend of the data but on average overestimates the transparency for all four nuclear targets. The increase of T_A, which we see at high Q^2 in this scenario, is driven by the $(t - t_F)$ factor in Eq. (5) and the time dilatation effect seen in Figure 5. The latter results in an increase of t_F as a function of Q^2 in the target rest frame or, equivalently, the π^+ three momentum.

To show the effect of time dilatation alone we take in Eq. (5) the pedestal value $X_0 = r_{\rm lead} = 1/2$ independent of Q^2. The result of this assumption is shown by the solid curves and provides a good agreement with data. However, there is an interplay between the formation times used and the Q^2–dependent pedestal value in the effective cross section, see Eq. (5). Either a larger pedestal value or a decreased t_F would lower the dash–dotted line in Figure 6 toward the data. We note that the scenario leading to the solid curve (no Q^2 dependence) is different from that in Refs. [21, 22] where a Q^2–dependent pedestal value had been used.

The calculations of Refs. [21, 22] show a pronounced CT effect already at values of Q^2 as low as 1.1 GeV^2. In these works it was assumed that *all* produced π^+ are subject to CT, whereas in our model the π–pole mechanism, which at low Q^2 gives the dominant contribution to the forward production of π^+, is not affected by the formation time effect. To model this situation we assume the same t_F for all pions produced by the longitudinal and transverse photons. In Figure 6 (left, top panel) the result of such a calculation is shown by the dash–dash–dotted curve; it is seen to strongly overestimate the transparency ratio. Thus, assuming a finite t_F also for preexisting pions which are knocked out from the nucleon meson cloud (t–channel process) will destroy the agreement obtained above. The fact that the calculations of Refs. [21, 22] do fit the data is due to the facts that there 1) the *formation* times of (pre)pions in the laboratory, essentially free parameters in [21, 22], are smaller than those extracted from the Lund model and 2) in Ref. [21] the total cross section was used in the Glauber attenuation formula. The latter may be a good approximation for the strictly forward kinematics in this experiment where any elastic process would scatter the pion out of the forward acceptance. However, because of the finite experimental resolution and the acceptance cuts [27] around the central values of the pion three momentum (see Table I), the ideal forward kinematics is not realized in the πCT experiment. As a result the attenuation in the πCT experiment is not driven necessarily by the total π^+N cross section.

So far we have considered the (pre)hadronic expansion times extracted from the string breaking pattern of the Lund model. In Figure 7 we present the results with t_F calculated when using Eq. (3) – the concept realized in Refs. [21, 22]. The calculations were done for $\Delta M = 1$ GeV as a fit parameter. This is an optimal value needed to reproduce the πCT data with our treatment of FSI. The dash–dash–dotted curves realize the CT effect in both the longitudinal and transverse channels and dash–dotted curves in the transverse channel only. In addition we show the results of the CT effect in the longitudinal channel only (dot–dot–dashed curves). As one can see the latter scenario is certainly ruled out by the present data. Because of the dominance of the transverse cross section at high values of Q^2, a use of different values of ΔM in a range discussed before does not change this result significantly. This is particularly interesting because presently the CT effect is expected to show up in the longitudinal channel [17].

Our results based on the Lund model hadronization scheme and L–T separated transparencies presented in Figure 7 suggest that CT shows up in the transverse part of the γ^*–nucleus cross section $\sigma_{\rm T}$. It would, therefore, be interesting to see the Q^2 dependence of L–T separated experimental cross sections for the transparency. The ongoing experiments at JLAB [41] may verify this conclusion.

In summary, in this work we have presented a calculation of the nuclear transparency of pions in the reaction $A(e,e'\pi^+)A^*$ off nuclei. The microscopic input for the primary interaction of the virtual photon with the nucleon describes both the transverse and the longitudinal cross sections. The coupled–channel BUU transport model has been used to describe the FSI of hadrons in the nuclear medium. The formation times of (pre)hadrons follow the time–dependent hadronization pattern of hard DIS processes. Our results are consistent with the JLAB data and show that a detailed understanding of the primary γ^*N interaction may be essential for a quantitative understanding (and proof) of CT. The L–T separated cross sections would be extremely useful for this aim. It would, furthermore, be interesting to extend the present analysis to $Q^2 \sim 10$ GeV^2, where the largest CT effects are predicted.

We gratefully acknowledge helpful communications and discussions with D. Dutta, R. Ent, H. Gao and G. Miller. We appreciate helpful discussions with O. Buss, T. Gaitanos and the GiBUU group.

This work was supported by BMBF.

[1] S. J. Brodsky and A. H. Mueller, Phys. Lett. B **206**, 685 (1988); L. L. Frankfurt, G. A. Miller, and M. I. Strikman, Comments Nucl. Part. Phys. **21**, 1 (1992).
[2] P. Jain, B. Pire and J. P. Ralston, Phys. Rept. **271**, 67 (1996).
[3] A. S. Carroll *et al.*, Phys. Rev. Lett. **61**, 1698 (1988).
[4] I. Mardor *et al.*, Phys. Rev. Lett. **81**, 5085 (1998).
[5] A. Leksanov *et al.*, Phys. Rev. Lett. **87**, 212301 (2001).
[6] J. L. S. Aclander *et al.*, Phys. Rev. C **70**, 015208 (2004).
[7] G. Garino *et al.*, Phys. Rev. C **45**, 780 (1992).
[8] T. G. O'Neill *et al.*, Phys. Lett. B **351**, 87 (1995).
[9] N. C. R. Makins *et al.*, Phys. Rev. Lett. **72**, 1986 (1994).
[10] D. Abbott *et al.*, Phys. Rev. Lett. **80**, 5072 (1998).
[11] K. Garrow *et al.*, Phys. Rev. C **66**, 044613 (2002).
[12] D. Dutta *et al.*, Phys. Rev. C **68**, 064603 (2003).
[13] M. R. Adams *et al.*, Phys. Rev. Lett. **74**, 1525 (1995).
[14] A. Airapetian *et al.*, Phys. Rev. Lett. **90**, 052501 (2003).
[15] D. Dutta *et al.*, Phys. Rev. C **68**, 021001 (2003).
[16] E. M. Aitala *et al.*, Phys. Rev. Lett. **86**, 4773 (2001).
[17] M. Strikman, arXiv:0711.1625 [hep-ph].
[18] B. Z. Kopeliovich *et al.*, Phys. Rev. C **65**, 035201 (2002).
[19] T. Falter, K. Gallmeister and U. Mosel, Phys. Rev. C **67**, 054606 (2003) [Erratum-ibid. C **68**, 019903 (2003)].
[20] B. Clasie *et al.*, Phys. Rev. Lett. **99**, 242502 (2007).
[21] A. Larson, G. A. Miller and M. I. Strikman, Phys. Rev **C 74**, 018201 (2006).
[22] W. Cosyn, M. C. Martinez and J. Ryckebusch, Phys. Rev. C **77**, 034602 (2008).
[23] G. R. Farrar *et al.*, Phys. Rev. Lett. **61**, 686 (1988).
[24] O. Buss *et al.*, Phys. Rev. C **76**, 035502 (2007).
[25] O. Buss *et al.*, arXiv:nucl-th/0703060.
[26] B. Krusche *et al.*, Eur. Phys. J. A **22**, 347 (2004).

[27] B. Clasie, Ph.D. Thesis, MIT, (2006).
[28] M. M. Kaskulov, K. Gallmeister and U. Mosel, Phys. Rev. D **78**, 114022 (2008), arXiv:0804.1834 [hep-ph].
[29] M. Vanderhaeghen, M. Guidal and J. M. Laget, Phys. Rev. C **57**, 1454 (1998); M. Guidal, J. M. Laget and M. Vanderhaeghen, Nucl. Phys. A **627**, 645 (1997).
[30] F. E. Close and N. Isgur, Phys. Lett. B **509**, 81 (2001).
[31] B. Andersson *et al.*, Phys. Rept. **97**, 31 (1983).
[32] T. Sjostrand *et al.*, JHEP **0605**, 026 (2006).
[33] C. Friberg and T.Sjostrand, Phys.Lett. B**492**, 123 (2000).
[34] V. Tadevosyan *et al.*, Phys. Rev. C **75**, 055205 (2007).
[35] T. Horn *et al.*, Phys. Rev. Lett. **97**, 192001 (2006).
[36] T. Horn *et al.*, arXiv:0707.1794 [nucl-ex].
[37] K. Gallmeister and T. Falter, Phys. Lett. B **630**, 40 (2005).
[38] For details of the GiBUU method see: http://gibuu.physik.uni-giessen.de/GiBUU
[39] K. Gallmeister and U. Mosel, Nucl. Phys. A **801**, 68 (2008).
[40] T. Mertens *et al.*, arXiv:0810.2678 [nucl-ex].
[41] H. Gao and D. Dutta, private communications